Catalytic pyrolysis/gasification of refuse derived fuel for hydrogen production and tar reduction: Influence of nickel to citric acid ratio using Ni/SiO_2 catalysts

Paula H. Blanco, Chunfei Wu, Jude A. Onwudili, Valerie Dupont, Paul T. Williams*

Energy Research Institute, University of Leeds, Leeds, LS2 9JT, UK

(*Corresponding author: Tel: #44 1133432504; Email: p.t.williams@leeds.ac.uk)

Abstract: Gasification technology is an attractive alternative for the thermal treatment of solid wastes, producing a high energy value hydrogen rich syngas. The presence of tar in the produced gas diminishes its quality and potential use in further processes; for this reason the reduction of tar in waste gasification is a major challenge. In this work the pyrolysis/gasification of refuse derived fuel (RDF) from municipal solid wastes, was investigated using a two-stage reaction system with Ni/SiO_2 catalysts prepared by a sol-gel method varying the citric acid concentration (CA). The fresh and reacted catalysts were characterised for surface area and pore size distribution, temperature programmed oxidation (TPO), and high resolution scanning electron microscopy (SEM). The effect of the nickel to citric acid ratio (Ni:CA) was evaluated in terms of the characteristics and performance of the Ni/SiO_2 catalysts. The results showed that the prepared Ni/SiO_2 catalysts exhibited a relatively high surface area and an increase in pore size distribution as the Ni:CA ratio was increased. The efficiency of the prepared catalysts on tar reduction and hydrogen production was examined during the pyrolysis/gasification of RDF; the results were compared with a blank experiment using a bed of sand. The tar fraction was quantified using gas chromatography/mass spectrometry (GC/MS). A low tar concentration of ~0.2 mg_{tar}/g_{RDF} was attained using the catalysts with Ni:CA ratios of 1:1 and 1:3; additionally a high hydrogen concentration (58 vol.%), and low CH_4 (2.2 vol.%) and C_2-C_4 concentrations (0.8 vol.%), were attained using the catalyst with a Ni:CA ratio of 1:3. A higher tar concentration of ~1.7 mg_{tar}/g_{RDF} was attained using the bed of sand, while the hydrogen production was remarkably decreased. The major tar compounds identified in the tar samples using the Ni/SiO_2 catalysts were phenol, cresols, naphthalene, fluorene, and phenanthrene.

Keywords: Tar; Nickel; Pyrolysis; Gasification; RDF

1 Introduction

The pyrolysis and/or gasification of solid wastes are regarded as promising technologies with the potential to produce a hydrogen rich syngas that can be catalytically converted into methanol, Fischer-Tropsch oils or other chemical products, and also can be used as a gaseous fuel [1-5]. One of the major issues during the gasification process is tar formation; tar is a mixture of aromatic and oxygen-containing compounds present in the produced gas excluding gaseous hydrocarbons (C_2-C_4) and benzene [6-8]. Due to its complex composition, tars tend to condense inside the gasifier, or gas engine or turbines resulting in several mechanical problems and thus reducing the efficiency of the gasification process [9-11]. Different methods to determine tar composition have been reported in the literature [12,13]; the state of the art method for offline tar sampling and analysis is the Tar Protocol CEN/TS 15439 by means of tar condensation in an organic solvent, followed by further gas chromatography analysis [14]. Similar methodologies have been used by Adegoroye and co-workers [15], and by Andersson and co-workers [16] to determine tar during the gasification process. Recent tar determinations have reported the use of optical methods based on laser induced systems [17], specifically fluorescence signals are applied with the flexibility of achieving in-situ or online tar measurements; however the elevated cost of this technology might reduce its further application, compared with the Tar Protocol [12,13]. Besides the tar collection and determination, further methods to reduce tar content in the produced gas have been also analysed [18-21]. For example, different catalysts are commonly used during the catalytic steam reforming process, as some of them exhibit high activities for tar elimination and gas upgrading during the gasification process [8]. A range of catalysts such as olivine, dolomite, alkali metal, and novel catalysts have been investigated in relation to tar reduction, but nickel based catalysts have been more extensively studied for tar removal due to their low cost compared with catalysts such as Rh, Ru or Pt; due to its efficiency for C-C bond rupture [8,22] and relatively high activity during the catalytic steam reforming processes [23,24]. Catalytic performance during steam reforming has been evaluated according the nature of the catalysts, the Ni precursor, and the preparation method [23]; however the catalytic activity for hydrogen production and tar reduction has also been related to the type of catalytic support. A variety of mixed oxides (i.e. Al_2O_3, ZrO_2, TiO_2 and SiO_2) have been investigated as supports for nickel based catalysts due to their efficiency during the gasification process [25]. For example Li et al [26], used a tri-metallic catalyst (Ni-La-Fe/Al_2O_3) during the gasification of municipal solid wastes, resulting in high hydrogen and gas yields. Kim et al [27], prepared and characterised different Ni-alumina catalysts to be tested during the partial oxidation of

methane into syngas; they found strong metal-support interactions and a good nickel particle dispersion. Goncalves et al [28], worked on the preparation of nickel catalysts based on alumina, silica and titania by a sol-gel method; they found higher surface areas using SiO_2 as support. Wu and Williams [29], used a series of nano-Ni/SiO_2 catalysts during the steam-reforming of ethanol for hydrogen production, reporting results for both catalysts properties and activity.

Different preparation methods such as impregnation and sol-gel have been used to synthesize the supported catalysts, in order to identify their effects in relation to catalyst properties and activity. For example Tomiyama et al [30], compared the characteristics and catalytic performance of Ni/SiO_2 catalysts prepared by homogeneous precipitation derived from a sol-gel process (HPG) and a conventional incipient wet impregnation method; they found a more efficient performance using the HPG prepared catalyst. Also Wu and Williams [21], worked on the comparison of Ni/SiO_2 catalysts prepared by sol-gel and impregnation methods; the catalysts were tested for their efficiency for hydrogen production during the steam reforming of ethanol, obtaining better results for the sol-gel catalyst. The effects of using different raw materials during the catalysts preparation has been previously studied due to its influence on catalyst characteristics such as surface area and mesoporous formation. For example, the change in the citric acid used for the silica wet gel formulation has been previously analysed by Takahashi et al [31], for the formation of mesoporous amorphous silica. The influence of nickel to citric acid ratio during the sol-gel preparation of Ni/SiO_2 catalysts has been previously analysed, and influenced the catalyst performance for hydrogen production during the steam reforming of ethanol [29]. Modifications of catalyst properties such as nickel dispersion and mesoporous volume have also been investigated [32].

In the present work a series of Ni/SiO_2 catalysts were tested for the catalytic pyrolysis/gasification of refuse derived fuel (RDF), using a two-stage reactor system. The effects of varying the nickel to citric acid (CA) ratio (Ni:CA) in relation to the catalyst properties were analysed. The tar composition and hydrogen production obtained using the Ni/SiO_2 catalysts were compared with those results obtained for blank experiments using a bed of sand instead of catalyst during the gasification stage.

2 Materials and Experimental

2.1 Materials

Municipal solid waste in the form of Refuse Derived Fuel (RDF) pellets, with a particle size of ~1.0 mm were used in this work as the raw feedstock material. Details about the

elemental analysis can be found in our previous work [22], however the general composition reported was about 43wt.% of carbon (C), 6wt.% of hydrogen (H), 32wt.% oxygen (O) and about 0.5wt.% of nitrogen (N). In addition, the proximate analysis of the RDF was; 7% moisture content, 15% of ash content and about 67% of volatile matter. Three Ni/SiO_2 catalysts with different Ni:CA molar ratios and 20 wt.% of nickel content, were prepared by a sol-gel method. The preparation details can be found elsewhere [21], however a brief description is given; $Ni(NO_3)_2 \cdot 6H_2O$ (Sigma-Aldrich), and anhydrous citric acid (Alfa Aesar) were dissolved into 200 ml, and stirred at 60 °C for 3 hours. A solution of different volumes of deionised water and 50 ml of absolute ethanol were added; then a fixed amount of tetraethoxysilane (TEOS; Sigma-Aldrich) was dropped into the solution; the solution was stirred for 30 minutes at 60 °C and then dried at 80 °C overnight, and finally calcined at 500 °C for 4 hours in the presence of air (20 °C min^{-1} heating rate). The catalysts were assigned as Ni/SiO_2-A, Ni/SiO_2-B, and Ni/SiO_2-C for the Ni:CA ratios of 1:1, 1:2, and 1:3 respectively. All the catalysts were crushed and sieved to obtain particles with a size between 0.050 mm-0.180 mm; the same particle size was used for the sand in the blank experiments carried out using the bed of sand. The catalysts were activated in the reactor by preheating the gasification stage at 800 °C, under a nitrogen atmosphere. None of the catalysts were reduced as the produced gases such as H_2 and CO were able to reduce the catalyst within the reactor.

2.2 Catalysts testing with pyrolysis-gasification of refuse derived fuel

The prepared catalysts were tested for their efficiency in relation to hydrogen production and tar reduction during the pyrolysis/gasification of refuse derived fuel (RDF), using a two-stage reaction system. A schematic diagram of the reactor is shown in Figure 1; the reaction system used was a small scale two-stage batch reactor, constructed of stainless steel and ceramic is used as insulation material; the total height of the reactor was 55cm including both stages. Both electrical furnaces were controlled independently; additionally two thermocouples were used to keep the desired temperatures at each stage. The water supply system and nitrogen inlets are located at the top of the reactor. About 2 grams of the RDF sample were placed within the first pyrolysis stage, whereas in the second gasification stage, about 1 gram of catalyst (or sand) was used as catalyst bed, with a catalyst:RDF ratio of 1:2 [22]. The gasification stage was preheated at 800 ºC in order to activate the catalyst, and at the same time the pyrolysis stage was preheated up to 220 ºC, before the RDF decomposition temperature (230 ºC) [33]. Once both temperatures were stable, a water pump was turned on to inject water and provide steam into the reactor with a flow rate of 5 ml h^{-1}; additionally the

pyrolysis temperature was increased to 600 ºC with a heating rate of 30 ºC min^{-1}. The total amount of water supplied was around 3.5 ml; thus the steam to RDF ratio was 1.75:1.0 considering about 40 minutes of water injection during RDF conversion. Nitrogen with a flow rate of about 80 ml min^{-1} was used to carry the pyrolysis gases through to the second gasification stage. When the desired temperatures were reached, the reactor was maintained under these conditions for a further 30 minutes. The produced gases were passed through a cooling system; the non-condensable gases were collected in a gas sample bag, and the condensable fraction was collected in two condensers cooled by air and dry-ice respectively.

The produced gases were analysed by packed column gas chromatography (GC) in order to calculate light hydrocarbons (C_2-C_4) and permanent gases (H_2, CO, N_2, O_2, CO_2) contained in the produced gas. A brief description of the GC analysis is as follows. A Varian CP-3380 gas chromatograph with a flame ionization detector (GC/FID), provided with a column packed with 80-100 mesh Hysep and using nitrogen as carrier gas, was used to analyse hydrocarbons (C_2-C_4). Permanents gases were analysed in a separate CP-3380 gas chromatograph with two packed columns each one with a thermal conductivity detector, and using argon as carrier gas. One column was packed with a 60-80 mesh molecular sieve, and was used to analyse H_2, CO, N_2 and O_2; the second column was packed with 80-100 mesh, and was used to analyse CO_2.

The general mass balance was calculated considering the initial sample weight, the steam added along the experiment; the final gas amount, the tar/oil fraction collected and the solid (char) remaining after the experiment; the general equation used is as follows:

$$mass\ balance = \frac{gas\ products + liquid\ products + char\ (residue)}{RDF + Supplied\ water} \qquad \text{Eq (1)}$$

2.2.1 Tar analysis

The condensed fraction from the produced gases was collected in the condenser system and recovered using dichloromethane (DCM, analytical reagent grade, Fischer Scientific) as solvent. A two phase heterogeneous fraction was obtained containing a water fraction and a tar/oil mixed with DCM fraction. Both fractions were physically separated by simple decantation. A bed of sodium sulphate (Na_2SO_4) was prepared by placing the salt in the oven for 2 hours at 140 ºC, and then the tar/oil with DCM fraction was passed through the bed in order to remove any water traces. After this, the volumes of the resulting solution were matched by evaporating the DCM contained in the samples at very low boiling point using a

Genevac Evaporation system. The tar composition and quantification was carried out using a mass spectrometer Varian CP-3800 gas chromatograph coupled with a Varian Saturn 2200 GC/MS/MS. 2 micro litres of each sample were injected into the injector port, whose temperature was 290 ºC. The oven programme temperature was 40 ºC for 2 minutes then ramped up to 280 ºC with 5 ºC min^{-1} heating rate, and finally this temperature was held for 10 more minutes. The transfer line temperature was 280 ºC, manifold at 120 ºC, and 200 ºC for the trap temperature. A 3-point calibration curve was obtained using a mixed standard solution containing polyaromatic hydrocarbons (PAHs) and oxygenated compounds.

2.2.2 Catalysts Characterization

The fresh Ni/SiO_2 catalysts were characterised to obtain their BET surface area, total pore volume and pore size data, using a Quantachrome NOVA 2200e series surface area and pore analyzer. The fresh catalysts were degassed under a nitrogen atmosphere at 120 ºC for about 2 hours, after that the N_2 adsorption and desorption isotherms were obtained at 77K. The specific surface area was calculated from the adsorption curve, using the Multipoint Brunauer, Emmett & Teller (BET) equation. The micropore and mesoporous volume were calculated from the desorption curve according to the Dubinin-Radushkevich (DR) method. The total pore volume and pore diameter were calculated using the Barrett, Joyner & Halenda (BJH) method.

After the pyrolysis/gasification of RDF, the reacted catalysts were analysed by temperature programmed oxidation (TPO), using a Stanton-Redcroft thermogravimetric analyzer (TGA). About 20 mg of each catalyst were placed in a pan and heated under an air atmosphere up to 800 ºC with 15 ºC min^{-1} heating rate, with 10 min holding time. The differential thermogravimetric (DTG-TPO) curves were also obtained and discussed in this work. High-resolution scanning electron microscopy (SEM) images of reacted Ni/SiO_2 catalysts morphology were obtained using a LEO 1530 apparatus.

3 Results and Discussion

3.1 Characterization of Fresh Catalysts

The BET (Brunauer, Emmet and Teller) surface area and porosity characteristics of the prepared Ni/SiO_2 catalysts were determined by N_2 adsorption-desorption; the results obtained are presented in Table 1. From Table 1 it can be seen that surface areas of the Ni/SiO_2 catalysts were very high; for example, the surface area values were increased from about 550 m^2 g^{-1} for the Ni/SiO_2-A catalyst (Ni:CA ratio of 1:1), to more than 700 m^2 g^{-1} for the

Ni/SiO_2-B and Ni/SiO_2-C catalysts with a nickel to citric acid ratio (Ni:CA) of 1:2 and 1:3 respectively. The similar values of surface area observed for the catalysts prepared with 1:2 and 1:3 Ni:CA ratios might be due to the higher presence of citric acid generates polymeric networks rather than particle aggregates; the higher CA the higher swelling of the wet silica gel occurred [31]. Also the amount of citric acid used during the preparation, altered the pH of the solution which would also influence nickel aggregation and hence the formation of SiO_2 particles.

The micropore and mesoporous volumes of the catalysts were obtained using the Dubinin-Radushkevich (DR) method; whereas the total pore volume and the pore diameter were obtained using the Barrett, Joyner & Halenda (BJH) method. Table 1 shows that the mesoporous volumes obtained for the Ni/SiO_2 catalysts were increased as the Ni:CA ratio increased. For example the mesopore volume of the Ni/SiO_2-A catalyst (Ni:CA of 1:1) was 0.09 $cm^3\ g^{-1}$ and increased up to 0.6 $cm^3\ g^{-1}$ for the Ni/SiO_2-C catalyst (Ni:CA of 1:3).

Considering the pore diameter values obtained for all the catalysts, it can be noted that all are considered as mesoporous materials since the values are within 2-50 nm [34]. It can also be noted that as the Ni:CA ratio was increased, the total pore volume and pore diameter increased; this can be related with the increased citric acid used during the preparation method, as the Ni loading remained constant for all the prepared catalysts (20 wt.%). Takahashi et al [32], reported a direct relation between the volume of citric acid used and the pore volume obtained in the Ni/SiO_2 catalysts. The increase in the pore diameter as the Ni:CA was increased, was explained due to a higher shrinkage, this suggests that the initial spaces occupied by the citric acid turned into pores after the citric acid elimination during the calcination process; this increase in the pore size might also indicate that the citric acid is well dispersed in CA-silica composites in the form of nanocomposites [31]. The lowest pore diameter (3.8 nm) was observed for the Ni/SiO_2-A catalyst, while the highest pore diameter ca. 7 nm was obtained for the Ni/SiO_2-C catalyst with a Ni:CA of 1:3.

The adsorption-desorption isotherms were determined for the fresh catalysts; the curves are presented in Figure 2. From Figure 2 it can be noted that the hysteresis loop characteristic of each isotherm was displaced slightly to higher pressures into the multilayer region of the isotherm as the mesoporous volume and pore diameter were increased (Table 1). The isotherm of the Ni/SiO_2-A catalyst (Ni:CA 1:1) appears to be a combination of the adsorption type I and type IV isotherms based on the classification suggested by the International Union of Pure & Applied Chemistry (IUPAC) [34]. This combination could suggest an isotherm from a solid with a limited pore size and very small external surface area; also the hysteresis

loop (H_2-type) indicates a complex pores structure and a network with pores of different shapes and sizes [35]. The isotherms for the Ni/SiO_2 catalysts with Ni:CA ratios of 1:2 and 1:3 were characterised as isotherms of the type IV, this type of isotherm is generally associated with the filling and emptying of mesopores by capillary condensation; the hysteresis loop observed in the multilayer region is of the H_1-type produced by adsorbents with narrow distribution of uniform pores [35].

3.2 Ni/SiO_2 catalysts with pyrolysis/gasification of RDF

3.2.1 Mass Balance and Gas Analysis

The mass balance for the pyrolysis/gasification of RDF with different catalysts and sand is presented in Table 2. The gas yield was calculated as the weight of produced gas divided by the initial weight of RDF used (Eq. 1). The residue yield was calculated as the weight of residue after pyrolysis of RDF divided by the initial sample weight. From Table 2, it was noted that for all the experiments a RDF in the first stage pyrolysis that a conversion to char of around 30 wt.% was obtained, which was as expected since for all the experiments, the pyrolysis conditions of the RDF in the first stage were maintained.

Only 50 wt.% of gas yield was obtained for the experiment without catalyst; whereas the gas yield was significantly increased to 70 wt.% in the presence of the Ni/SiO_2 catalyst (Table 2). Regarding the results of hydrogen production using the bed of sand as the blank experiment, only 24 vol.% of H_2 concentration was obtained, whereas the H_2 concentration was increased significantly to 57 vol.% in the presence of the Ni/SiO_2 catalyst (Table 2). The CO concentration was ~18 wt.% for the experiments carried out with catalysts, while a concentration of ~22 wt.% was obtained using the bed of sand. According to Le Chatelier's principle, the increase in the concentration of both H_2 and CO can be influenced by reactions such as steam reforming and water-gas (Reactions 1 and 5, Table 3), additionally an increase in hydrogen produced might be explained by the enhancement of cracking reactions (Reactions 3 and 4, Table 3) [36]. In addition, by using the bed of sand, much higher concentrations for CH_4 and C_2-C_4 were obtained, highlighting the promotion of tar cracking by using Ni/SiO_2 catalysts.

For the experiments carried out using the Ni/SiO_2 catalysts, the gas yield was around 70 wt.% with the change of the Ni:CA ratio from 1:1 to 1:3, indicating that there is little influence of the content of citric acid in the preparation of the Ni/SiO_2 catalysts on the gas production from the pyrolysis/gasification of RDF process. For the gas composition derived from the pyrolysis/gasification of RDF in the presence of the Ni/SiO_2 catalyst, the H_2

concentration was similar at ~58 vol.% with an increase in the Ni:CA ratio from 1:1 to 1:3. On the other hand, the concentration of CH_4 was reduced from 3.1 to 2.2 vol.% and the C_2-C_4 were also reduced from 1.3 to 0.8 vol.% by increasing the CA concentration from 1:1 to 1:3; this effect might be due to the promotion of cracking reactions (Reactions 3 and 4, Table 3), at higher citric acid content.

Wu et al [29], have previously studied Ni/SiO_2 catalysts for their efficiency on hydrogen production during the ethanol steam reforming process; their results demonstrated an increase in both hydrogen production and gas yield as the nickel to citric acid ratio was increased from 1:0.5 to 1:1 in Ni/SiO_2 catalysts, it was also observed that further increase in the Ni:CA ratio resulted in lower increases in the gas yield [29].

From Table 2 it was also observed that the CO_2 concentration was similar at ~20 vol.%, by modifying the Ni:CA ratio (Ni/SiO_2- A, B, C), a similar CO_2 concentration was obtained using the bed of sand. This affinity might be related with a similar promotion of the water-gas shift reaction (Reaction 5, Table 3). Regarding the CH_4 and C_2-C_4 concentrations a reduction trend was also observed as the Ni:CA was increased for the Ni/SiO_2-A, B, and C sol-gel catalysts. This effect can be due to the promotion of hydrocarbons decomposition and reforming reactions (1-5, Table 3); followed by a release of H_2, and hence an increase in its concentration [37].

3.3 GC/MS Tar Analysis

The collected tar samples from the condensation system were analysed using GC/MS/MS, the assigned compounds, elution retention time, molecular weight, compound concentration ($\mu g_{compound}/g_{RDF}$), and global tar concentration values (mg_{tar}/g_{RDF}), are shown in Table 4. From Table 4 it can be observed that the major contributions for all the analysed tar samples came from the phenol, cresols, naphthalene, fluorene and phenanthrene compounds. The highest tar concentration of 1.7 mg_{tar}/g_{RDF} was attained using the bed of sand; whereas significant improvement in tar decomposition was attained using the Ni/SiO_2 catalysts, reducing up to 0.15 mg_{tar}/gRDF.

Researchers have grouped tar compounds into five classes, based on the molecular weight and characteristics of the identified compounds, as shown in Table 5 [38,39]. All the identified tar compounds in this work were grouped from Class 2 to Class 5; tar Class 1 is not included on Table 5 as it is always referred to as non-GC detectable compounds. Figure 3 shows the concentrations for each tar Class; it can be noted that for all the analysed samples, the most abundant groups are Class 2 and Class 4, whereas lower concentrations of tar Class

3 and Class 5 were observed. Also the high catalytic activity for tar cracking is observed by using the Ni/SiO_2 catalysts, compared with the blank experiment carried out with the sand bed, under the same experimental conditions.

Different major tar compounds such as styrene, phenol, naphthalene and phenanthrene, have been identified in tars from the catalytic steam reforming of RDF and biomass [22,38, 40,41]. The tar Class 2 includes heterocyclic aromatic compounds; within this group the most notable compound was phenol which showed the highest concentration ranging from 62 up to 613 $\mu g_{phenol}/g_{RDF}$ (Table 4). In order to predict the reduction of heterocyclic tars using different catalysts, sometimes phenol has been referred to as a tar model compound due to its major presence in tar samples [42,43]. From Table 4 it can be noted that the Ni/SiO_2-A catalyst, prepared with a Ni:CA of 1:1, showed a significant catalytic activity for phenol conversion with a concentration of 62 $\mu g_{phenol}/g_{RDF}$, while low phenol conversion (ca. 613 $\mu g_{phenol}/g_{RDF}$) was obtained using the sand bed. The formation mechanism of aromatic hydrocarbons such as naphthalene and (methyl)indenes has been previously reported by Larsen et al. [44]. The cyclopentadienes resulting from the decarbonylation reaction undergoes to a Diels-Alder reaction leading in the dimer formation. The system is then rearranged by further loss of hydrogen leading to the formation of naphthalene and indenes. This elucidates that phenol is the precursor for the naphthalene and (methyl)indenes, during the pyrolysis process (Figure 4).

From Figure 3 it can be noted a reduction in the concentration of tar Class 3 by increasing the Ni:CA ratio from 1:1 to 1:2, however a slight increase was noted using the Ni/SiO_2-C catalyst with a Ni:CA ratio of 1:3; this might be related to the cracking properties of the catalyst as the higher citric acid concentrations avoided the rupture of lighter compounds (1-Ring), whereas more efficient catalytic activities might be present for higher aromatic compounds.

Within the tar Class 4, naphthalene and their methyl derivatives can be found along with phenanthrene, biphenyl and fluorene (Table 5). A remarkable reduction in the concentration of tar Class 4 was observed (Figure 3) by increasing the Ni:CA ratio from 1:2 (Ni/SiO_2-B) to 1:3 (Ni/SiO_2-C); this reduction might be due to the higher concentration of citric acid which promoted higher pore volume and pore diameters in the catalysts (Table 1), which at the same time might have allowed larger molecules to be reformed by passing into the catalyst pore structure [29].

The Class 5 tar concentration was very low for the experiments carried out with the catalyst bed, ranging from ca. 6 up to 9 $\mu g_{tar\text{-}Class5}/g_{RDF}$. Matas Guell et al [43], reported that

despite the very low concentration of this tar Class 5, it seems to dominate the overall tar dew point which is highly relevant for the associated tar problems with the use of the product gas downstream. From the analysed samples the more notable compounds were fluoranthene and pyrene for this tar Class 5. For the sand experiment, the lowest tar concentration was also related to this Class 5, with a value of 9 $\mu g_{tar\text{-}Class5}/g_{RDF}$.

The major identified compounds in all the analysed tar samples were: phenol, cresols, naphthalene, fluorene and phenanthrene (Table 4). The catalytic activity for phenol and cresols was as follows: Ni/SiO_2-A > Ni/SiO_2-C > Ni/SiO_2-B; for naphthalene and fluorene: Ni/SiO_2-C > Ni/SiO_2-A > Ni/SiO_2-B; and for phenanthrene Ni/SiO_2-C > Ni/SiO_2-A > Ni/SiO_2-B. Thus, considering the previous trend, it seems that Ni/SiO_2-C catalyst presented the best performance in terms of major tar compounds reduction, although final tar concentrations of 0.2 mg_{tar}/g_{RDF} was attained using both Ni/SiO_2-A and Ni/SiO_2-C catalysts.

3.4 Characterization of Reacted Catalysts

The coke deposition over the reacted Ni/SiO_2 catalysts was investigated by thermogravimetyric analysis (TGA); temperature programmed oxidation curves (TGA-TPO), and their respective derivative curves (DTG-TPO) are presented in Figure 5. Different stages of weight changes can be identified along the TGA curves at different temperatures.

In Figure 5, a comparison of the TGA-TPO and DTG-TPO curves of the reacted catalysts at different Ni:CA ratios is shown. The TGA-TPO curves present an initial weight reduction around 100 °C, that might be associated with moisture evaporation [29]; after that an increase in the weight percentage is observed from 350 °C up to 600 °C, and finally a weight decrease was observed. The analysis of the DTG-TPO curves show a region with a weight increase between 300 °C and 400 °C which might be associated with nickel oxidation. The DTG-TPO curves presented similar trends which might indicate that a similar type of carbon was deposited over the reacted catalysts surface; for example the major oxidation peaks around 650 °C are suggested to be due to the oxidation of filamentous type carbon, whereas the peaks around 500 °C were ascribed to the oxidation of amorphous carbons [45,46]. Analysing the surface of the reacted catalysts by scanning electron microscopy (SEM), some filamentous carbon type could be observed for the reacted catalysts (Figure 6). Similar observations have been previously reported by Wu et al. [29], while analysing reacted catalysts prepared varying the Ni to CA ratio. Coke deposition as observed in this work, often leads to catalyst deactivation, primarily due to masking of catalyst active sites [46,48]. Although, catalyst re-use was not attempted in this work, generally, a decrease in catalytic

activity would be expected due to amount and type of carbon deposits found on the catalyst surface. Further experimental work on the extensive re-use of catalysts will be carried out to investigate the effect of catalyst surface masking on the overall RDF gasification process.

4 Conclusions

The catalytic pyrolysis/gasification of refuse derived fuel (RDF) has been investigated using Ni/SiO_2 catalysts prepared by a sol-gel method varying the citric acid concentration. Analysis of the prepared catalysts showed that they were mainly mesoporous and the pore volume, and pore diameter were increased as the citric acid was increased in the Ni/SiO_2 catalysts sol-gel preparation.

The higher H_2 content in the gas produced from pyrolysis/gasification of the RDF was around 58 vol.%, obtained using Ni/SiO_2 catalysts with Ni:CA ratios of 1:2 and 1:3 respectively; whereas methane and C_2-C_4 concentrations were reduced in the produced gas as the Ni:CA ratio was increased.

Low tar concentrations of 0.2 mg_{tar}/g_{RDF} were obtained using the Ni/SiO_2-A and Ni/SiO_2-C catalysts prepared with a Ni:CA of 1:1 and 1:3 respectively. The major tar compounds identified were phenol, cresols, naphthalene, fluorene, and phenanthrene; the highest tar cracking activity for these compounds was observed for the Ni/SiO_2-C catalyst (Ni:CA, 1:3).

Filamentous carbons were found to be formed over the reacted catalysts. The amount and type of carbons deposited on the reacted catalyst were found to be only slightly influenced by the changing of the citric acid for the preparation of the Ni/SiO_2 catalysts.

The experiment carried out in the absence of a catalyst, (using sand in place of catalyst) exhibited very high tar concentrations of 1.7 mg_{tar}/g_{RDF} compared with the experiments carried out with catalysts, while the gas composition and gas yield were remarkably diminished.

Acknowledgements

The authors would like to thank the National Council of Science and Technology of Mexico (Conacyt) for a scholarship of one of us: PHB. Funding from the UK Science & Engineering Research Council (Grant EP/G036608/1) is also gratefully acknowledged.

References

1. Choudhary, T.V., Choudhary, V.R.: Energy-efficient syngas production through, catalytic oxy-methane reforming reactions. Angew Chem Int Edit **47**(10), 1828-1847 (2008). doi:DOI 10.1002/anie.200701237
2. Edwards, P.P., Kuznetsov, V.L., David, W.I.F.: Hydrogen energy. Philosophical Transactions of the Royal Society A: Mathematical, Physical and Engineering Sciences **365**(1853), 1043-1056 (2007). doi:10.1098/rsta.2006.1965
3. Dalai, A.K., Batta, N., Eswaramoorthi, I., Schoenau, G.J.: Gasification of refuse derived fuel in a fixed bed reactor for syngas production. Waste Management **29**(1), 252-258 (2009). doi:10.1016/j.wasman.2008.02.009
4. Belgiorno, V., De Feo, G., Della Rocca, C., Napoli, R.M.A.: Energy from gasification of solid wastes. Waste Management **23**(1), 1-15 (2003). doi:Doi: 10.1016/s0956-053x(02)00149-6
5. Li, J.F., Liao S.Y., Dan W.Y., Jia K.L., Zhou X.R. Experimental study on catalytic steam gasification of municipal solid waste for bioenergy production in a combined fixed bed reactor. Biomass & Bioenergy, 46, 174-180, (2012).
6. Devi, L., Ptasinski, K.J., Janssen, F.J.J.G.: A review of the primary measures for tar elimination in biomass gasification processes. Biomass and Bioenergy **24**(2), 125-140 (2003). doi:Doi: 10.1016/s0961-9534(02)00102-2
7. Neeft, J.P.A., Knoef, H.A.M., Onaji, P., Nederland, S.E.C., Group, B.B.T.: Behaviour of Tar in Biomass Gasification Systems: Tar Related Problems and Their Solutions. Novem, (1999)
8. Abu El-Rub, Z., Bramer, E. A., Brem, G. : Review of Catalysts for Tar Elimination in Biomass Gasification Processes. Industrial and Engineering Chemistry Research **43**(22), 6911-6919 (2004).
9. Caballero, M.A., Corella, J. Aznar, M. P. Gil, J.: Biomass gasification with air in fluidized bed. Hot gas cleanup with selected commercial and full-size nickel-based catalysts. Industrial and Engineering Chemistry Research **39**(5), 1143-1154 (2000).
10. Miccio, F., Moersch, O., Spliethoff, H., Hein, K.R.G.: Generation and conversion of carbonaceous fine particles during bubbling fluidised bed gasification of a biomass fuel. Fuel **78**(12), 1473-1481 (1999).
11. Li, C., Suzuki, K.: Tar property, analysis, reforming mechanism and model for biomass gasification--An overview. Renewable and Sustainable Energy Reviews **13**(3), 594-604 (2009). doi:DOI: 10.1016/j.rser.2008.01.009
12. Simell, P., Ståhlberg, P., Kurkela, E., Albrecht, J., Deutsch, S., Sjöström, K.: Provisional protocol for the sampling and analysis of tar and particulates in the gas from large-scale biomass gasifiers. Version 1998. Biomass and Bioenergy **18**(1), 19-38 (2000). doi:10.1016/s0961-9534(99)00064-1
13. Neeft, J.P.A., Knoef, H.A.M., Zielke, U., Sjostrom, K., Hasler, P., Simell, P.A.: Guideline for sampling and analysis of tar and particles in biomass producer gases In: Tar Protocol. ECN ERK-CT1999-2002, Pette, Nederland, (1999)
14. DD CEN/TS 15439 Biomass Gasification - Tar And Particles In Product Gases - Sampling And Analysis. In. CEN Technical Specification, (2006)
15. Adegoroye, A., Paterson, N., Li, X., Morgan, T., Herod, A.A., Dugwell, D.R., Kandiyoti, R.: The characterisation of tars produced during the gasification of sewage sludge in a spouted bed reactor. Fuel **83**(14-15), 1949-1960 (2004). doi:10.1016/j.fuel.2004.04.006

16. Andersson, K., Levin, J.-O., Nilsson, C.-A.: Sampling and analysis of particulate and gaseous polycyclic aromatic hydrocarbons from coal tar sources in the working environment. Chemosphere **12**(2), 197-207 (1983). doi:10.1016/0045-6535(83)90162-5
17. Baumhakl, C., Karellas, S.: Tar analysis from biomass gasification by means of online fluorescence spectroscopy. Optics and Lasers in Engineering **49**(7), 885-891 (2011). doi:http://dx.doi.org/10.1016/j.optlaseng.2011.02.015
18. Li, J., Yan, R., Xiao, B., Liang, D.T., Du, L.: Development of Nano-NiO/Al2O3 Catalyst to be Used for Tar Removal in Biomass Gasification. Environmental Science & Technology **42**(16), 6224-6229 (2008). doi:10.1021/es800138r
19. Sutton, D., Kelleher, B., Ross, J.R.H.: Review of literature on catalysts for biomass gasification. Fuel Process Technol **73**(3), 155-173 (2001). doi:Doi: 10.1016/s0378-3820(01)00208-9
20. Bangala, D.N., Abatzoglou, N., Martin, J.-P., Chornet, E.: Catalytic Gas Conditioning: Application to Biomass and Waste Gasification. Industrial & Engineering Chemistry Research **36**(10), 4184-4192 (1997). doi:10.1021/ie960785a
21. Wu, C.F., Williams, P.T.: A Novel Nano-Ni/SiO(2) Catalyst for Hydrogen Production from Steam Reforming of Ethanol. Environmental Science & Technology **44**(15), 5993-5998 (2010). doi:Doi 10.1021/Es100912w
22. Blanco, P.H., Wu, C., Onwudili, J.A., Williams, P.T.: Characterization of Tar from the Pyrolysis/Gasification of Refuse Derived Fuel: Influence of Process Parameters and Catalysis. Energy & Fuels **26**(4), 2107-2115 (2012). doi:10.1021/ef300031j
23. Park, H.J., Park, S.H., Sohn, J.M., Park, J., Jeon, J.-K., Kim, S.-S., Park, Y.-K.: Steam reforming of biomass gasification tar using benzene as a model compound over various Ni supported metal oxide catalysts. Bioresource Technology **101**(1, Supplement), S101-S103 (2010). doi:10.1016/j.biortech.2009.03.036
24. Taylor, A.D., DiLeo, G.J., Sun, K.: Hydrogen production and performance of nickel based catalysts synthesized using supercritical fluids for the gasification of biomass. Applied Catalysis B: Environmental **93**(1–2), 126-133 (2009). doi:10.1016/j.apcatb.2009.09.021
25. Sutton, D., Kelleher, B., Doyle, A., Ross, J.R.H.: Investigation of nickel supported catalysts for the upgrading of brown peat derived gasification products. Bioresource Technology **80**(2), 111-116 (2001).
26. Li, J., Liu, J., Liao, S., Zhou, X., Yan, R.: Syn-Gas Production from Catalytic Steam Gasification of Municipal Solid Wastes in a Combined Fixed Bed Reactor. In: International Conference on Intelligent System Design and Engineering Application 2010, pp. 530-534
27. Kim, P., Kim, Y., Kim, H., Song, I.K., Yi, J.: Synthesis and characterization of mesoporous alumina with nickel incorporated for use in the partial oxidation of methane into synthesis gas. Applied Catalysis A: General **272**(1–2), 157-166 (2004). doi:10.1016/j.apcata.2004.05.055
28. Goncalves, G., Lenzi, M. K., Santos, O. A. A., Jorge, L. M. M.: Preparation and characterization of nickel based catalysts on silica, alumina and titania obtained by sol-gel method. Journal of Non-Crystalline Solids **352**, 3697-3704 (2006).
29. Wu, C., Williams, P.T.: Hydrogen production from steam reforming of ethanol with nano-Ni/SiO2 catalysts prepared at different Ni to citric acid ratios using a sol–gel method. Applied Catalysis B: Environmental **102**(1–2), 251-259 (2011). doi:10.1016/j.apcatb.2010.12.005

30. Tomiyama, S., Takahashi, R., Sato, S., Sodesawa, T., Yoshida, S.: Preparation of Ni/SiO2 catalyst with high thermal stability for CO2-reforming of CH4. Applied Catalysis A: General **241**(1–2), 349-361 (2003). doi:10.1016/s0926-860x(02)00493-3
31. Takahashi, R., Sato, S., Sodesawa, T., Kawakita, M., Ogura, K.: High surface-area silica with controlled pore size prepared from nanocomposite of silica and citric acid. Journal of Physical Chemistry B **104**(51), 12184-12191 (2000). doi:Doi 10.1021/Jp002662g
32. Takahashi, R., Sato, S., Sodesawa, T., Suzuki, M., Ichikuni, N.: Ni/SiO2 prepared by sol-gel process using citric acid. Microporous and Mesoporous Materials **66**(2-3), 197-208 (2003). doi:DOI 10.1016/j.micromeso.2003.09.007
33. Buah, W.K., Cunliffe, A.M., Williams, P.T.: Characterization of Products from the Pyrolysis of Municipal Solid Waste. Process Safety and Environmental Protection **85**(5), 450-457 (2007). doi:DOI: 10.1205/psep07024
34. Sing, K.S.W., Everett, D.H., Haul, R.A.W., Moscou, L., Pierotti, R.A., Rouquerol, J., Siemieniewska, T.: Reporting Physisorption Data for Gas Solid Systems with Special Reference to the Determination of Surface-Area and Porosity (Recommendations 1984). Pure and Applied Chemistry **57**(4), 603-619 (1985).
35. Rouquerol, F., Rouquerol, J., Sing, K.S.W.: Adsorption by Powders and Porous Solids. Academic Press, London (1999)
36. Kim, J.-W., Mun, T.-Y., Kim, J.-O., Kim, J.-S.: Air gasification of mixed plastic wastes using a two-stage gasifier for the production of producer gas with low tar and a high caloric value. Fuel **90**(6), 2266-2272 (2011). doi:10.1016/j.fuel.2011.02.021
37. Pinto, F., André, R.N., Franco, C., Lopes, H., Gulyurtlu, I., Cabrita, I.: Co-gasification of coal and wastes in a pilot-scale installation 1: Effect of catalysts in syngas treatment to achieve tar abatement. Fuel **88**(12), 2392-2402 (2009). doi:10.1016/j.fuel.2008.12.012
38. Blanco, P.H., Wu, C., Onwudili, J.A., Williams, P.T.: Characterization and evaluation of Ni/SiO2 catalysts for hydrogen production and tar reduction from catalytic steam pyrolysis-reforming of refuse derived fuel. Applied Catalysis B: Environmental **134–135**(0), 238-250 (2013). doi:http://dx.doi.org/10.1016/j.apcatb.2013.01.016
39. Han, J., Kim, H.: The reduction and control technology of tar during biomass gasification/pyrolysis: An overview. Renewable and Sustainable Energy Reviews **12**(2), 397-416 (2008). doi:DOI: 10.1016/j.rser.2006.07.015
40. Wolfesberger-Schwabl, U., Aigner I., Hofbaur H., Mechanism of tar generation during fluidized bed gasification and low temperature pyrolysis, Industrial Engineering Chemistry Research, 51, 13001-13007 (2012). DOI: 10.1021/ie300827d
41. Hernandez, J.J., Ballesteros R., Aranda G., Characterisation of tars from biomass gasification: Effect of the operating conditions. Energy, 50, 333-342 (2013). doi.org/10.1016/j.energy.2012.12.005,
42. Abu El-Rub, Z., Bramer, E.A., Brem, G.: Experimental comparison of biomass chars with other catalysts for tar reduction. Fuel **87**(10-11), 2243-2252 (2008). doi:DOI: 10.1016/j.fuel.2008.01.004
43. Matas Güell, B., Babich, I.V., Lefferts, L., Seshan, K.: Steam reforming of phenol over Ni-based catalysts – A comparative study. Applied Catalysis B: Environmental **106**(3–4), 280-286 (2011). doi:10.1016/j.apcatb.2011.05.012
44. Larsen, E., Egsgaard, H., Pedersen, K., Zielke, U., Brandt, P.: Tar compounds in condensates from different types of gasifiers. In: Kyritsis, S. (ed.) 1st World Conference on Biomass for Energy and Industry, Sevilla, Spain, 5-9 June 2000 2000, p. 2137. James & James (Science Publishers) Ltd

45. Wu, C., Williams, P.T.: Hydrogen production by steam gasification of polypropylene with various nickel catalysts. Applied Catalysis B: Environmental **87**(3–4), 152-161 (2009). doi:10.1016/j.apcatb.2008.09.003
46. Wu, C., Williams, P.T.: Investigation of coke formation on Ni-Mg-Al catalyst for hydrogen production from the catalytic steam pyrolysis-gasification of polypropylene. Applied Catalysis B: Environmental **96**(1–2), 198-207 (2010). doi:10.1016/j.apcatb.2010.02.022
47. Devi, L., Ptasinski, K.J., Janssen, F.J.J.G.: Pretreated olivine as tar removal catalyst for biomass gasifiers: investigation using naphthalene as model biomass tar. Fuel Process Technol **86**(6), 707-730 (2005). doi:DOI: 10.1016/j.fuproc.2004.07.001
48. Wang C., Dou B., Chen H., Song Y., Xu Y., Du X., Zhang L., Luo T., Tan C., Renewable hydrogen production from steam reforming of glycerol by Ni–Cu–Al, Ni–Cu–Mg, Ni–Mg catalysts. International Journal of Hydrogen Energy, 38 (9), 3562-3571 (2013). http://dx.doi.org/10.1016/j.ijhydene.2013.01.042,

Table 1. Surface Properties of the Ni/SiO_2 catalysts

Catalyst	Ni content (wt%)	Ni:CA ratio	Surface area[1] ($m^2\ g^{-1}$)	Micropore volume[2] ($cm^3\ g^{-1}$)	Mesoporous volume[2] ($cm^3\ g^{-1}$)	Total pore volume[3] ($cm^3\ g^{-1}$)	Pore diameter[3] (nm)
Ni/SiO_2-A	20	1:1	547.50	0.270	0.090	0.150	3.818
Ni/SiO_2-B	20	1:2	788.20	0.390	0.363	0.548	4.312
Ni/SiO_2-C	20	1:3	756.40	0.389	0.602	0.884	6.608

[1] MultiPoint Brunauer, Emmett &Teller (BET) Method
[2] Dubinin-Radushkevich (DR) Method
[3] Barrett, Joyner & Halenda (BJH) Method

Table 2. Gas Composition, Product Yields and Mass Balance

Catalyst	Gas composition (Vol.%, N_2 free)					Gas Yield	Residue Yield	Mass Balance
	CO	H_2	CO_2	CH_4	C_2-C_4	(wt.%)	(%)	(wt.%)
Ni/SiO_2-A	17.7	56.6	21.3	3.1	1.3	71.1	29.5	96.3
Ni/SiO_2-B	18.8	57.8	20.1	2.4	0.9	71.2	30.3	93.7
Ni/SiO_2-C	18.4	57.9	20.7	2.2	0.8	68.7	29.8	91.6
Sand	22.3	24.3	20.7	19.0	13.7	50.0	30.5	96.5

Table 3. Reactions occurring during the second catalytic gasification stage [8,47]

Reaction Type	Reaction	
Steam Reforming	$C_nH_m + nH_2O \leftrightarrow nCO + \left(n + \frac{m}{2}\right) H_2$	(1)
Dry Reforming	$C_nH_m + nCO_2 \leftrightarrow 2nCO + \left(\frac{m}{2}\right) H_2$	(2)
Thermal cracking	$C_nH_m \leftrightarrow C^* + C_xH_y + gas$	(3)
Tars hydrocracking	$C_nH_m + H_2 \leftrightarrow CO + H_2 + CH_4 + \cdots + coke$	(4)
Water-gas shift reaction	$CO + H_2O \leftrightarrow CO_2 + H_2$	(5)

C_nH_m hydrocarbons representing tars. C_xH_y hydrocarbons representing lighter tars.

Table 4. GC/MS Tar Analysis

RT (min)	Assigned Peak	MW (g mol^{-1})	Ni/SiO_2-A	Ni/SiO_2-B	Ni/SiO_2-C	SAND
7.84	Furfural	96	—	5.39	1.52	28.77
7.81	Cyclopentanone	84	—	5.4	1.45	—
8.67	Ethylbenzene	106	—	—	—	16.75
9.02	p-Xylene	106	4.51	—	3.06	43.61
9.02	m-Xylene	106	4.42	—	3.18	42.11
9.86	Styrene	104	1.08	2.46	1.41	141.50
9.89	o-Xylene	106	—	—	—	11.95
12.45	Alphamethylstyrene	118	—	—	—	15.20
13.12	Betamethylstyrene	118	—	—	—	9.11
13.36	Phenol	94	61.68	255.09	183.82	613.56
14.78	s-Limonene	136	—	—	—	15.24
14.97	Indane	118	—	0.2	—	1.54
15.35	Indene	116	4.88	11.31	1.23	90.34
15.69	o-Cresol	108	2.07	6.82	2.72	36.10
16.14	Acetophenone	120	1.22	—	0.99	—
16.47	p-Cresol	108	3.53	16.2	5.58	65.16
16.48	m-Cresol	108	3.41	14.65	5.34	63.66
16.58	2-methoxyphenol	124	—	—	—	24.79
17.38	2-Methylbenzofuran	132	0.78	—	—	—
18.61	2,4-Dimethylphenol	122	—	—	—	5.63
19.27	Ethylphenol	122	—	—	—	13.59
19.27	2,6-Dimethylphenol	122	—	—	—	17.75
20.98	Naphthalene	128	19.14	79.2	4.11	58.18
20.98	2,3,5-Trimethylphenol	136	—	—	—	2.08
23.16	2-Methylnaphthalene	142	2.27	6.66	1.62	97.00
25.08	Biphenyl	154	2.06	4.61	2.06	69.20
25.32	2-ethylnaphthalene	156	—	—	—	—
25.54	2,6-dimethyl naphthalene	156	—	—	—	1.04
26.16	1,4-dimethylnaphthalene	156	—	1.43	1.21	0.95
27.47	Dibenzofuran	168	3.37	3.7	—	24.13
28.51	Fluorene	166	6.59	10.62	4.51	50.10
29.28	1,3-diphenylpropane	196	—	—	1.36	1.19
29.34	2-Phenylphenol	170	—	—	—	13.32
31.06	Phenanthrene	178	15.5	41.25	3.81	51.11
31.74	1-Phenylnaphthalene	204	—	—	—	1.40
31.97	o-Terphenyl	230	1.53	—	1.46	—
34.17	Fluoranthene	202	3.17	4.63	2.78	24.66
34.48	Pyrene	202	3.11	4.43	3.16	35.86
34.62	m-Terphenyl	230	2.64	2.82	2.49	29.99
41.98	1,3,5-triphenylbenzene	306	—	—	2.13	—
	Tar Concentration	($\mu g_{tar}/g_{RDF}$)	149.04	476.87	241.03	1716.52
	Tar Concentration	(mg_{tar}/g_{RDF})	**0.15**	**0.48**	**0.24**	**1.72**

Table 5. Classification of Tar Compounds identified by GC/MS

CLASS 2	CLASS 3	CLASS 4	CLASS 5
Heterocyclic Aromatics	**Aromatics 1-Ring**	**Light PAH 2-3 Rings**	**Heavy PAH 4-7 Rings**
Tars containing hetero atoms; highly water soluble compounds	Light hydrocarbons; do not pose a problem regarding condensability and solubility	Compounds that condense at low temperature even at very low concentration	Components that condense at high temperatures at low concentrations
Furfural	Ethylbenzene	Naphthalene	Fluoranthene
Cyclopentanone	p-Xylene	2-Methylnaphthalene	Pyrene
Phenol	m-Xylene	Biphenyl	1,3,5-Triphenylbenzene
o-Cresol	o-Xylene	2-ethylnaphthalene	
p-Cresol	Styrene	2,6-dimethylnaphthalene	
m-Cresol	Alphamethylstyrene	1,4-dimethylnaphthalene	
Acetophenone	Betamethylstyrene	Fluorene	
2-methoxyphenol	s-Limonene	1,3-diphenylpropane	
2-Methylbenzofuran		Phenanthrene	
2,4-Dimethylphenol		o-Terphenyl	
Ethylphenol		m-Terphenyl	
2,6-Dimethylphenol		Indane	
2,3,5-Trimethylphenol		Indene	
Dibenzofuran		1-Phenylnaphthalene	
2-Phenylphenol			

FIGURE CAPTIONS

Figure 1. Schematic diagram of the two-stage fixed-bed catalytic reactor

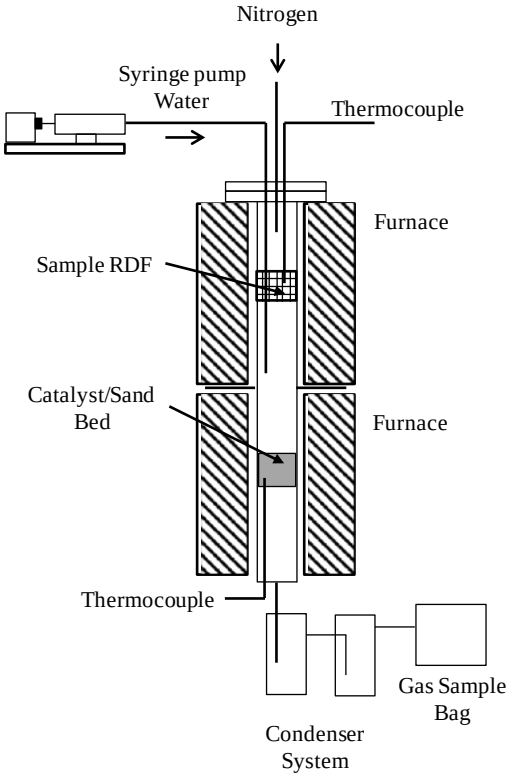

Figure 2. BET adsorption-desorption isotherms of fresh catalysts

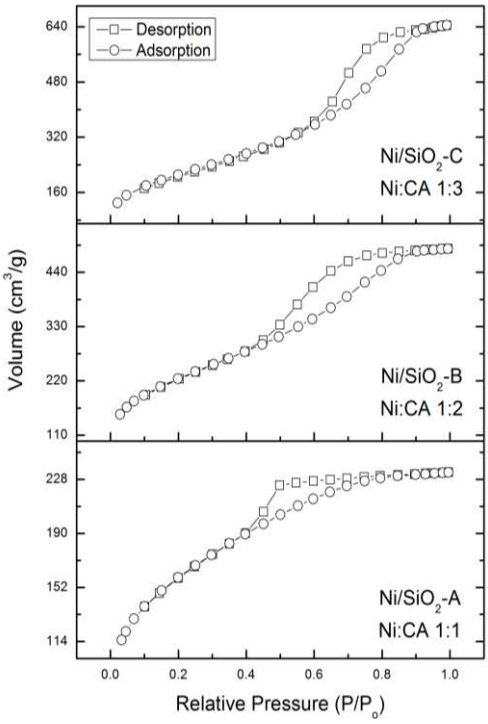

Figure 3. Tar Classification

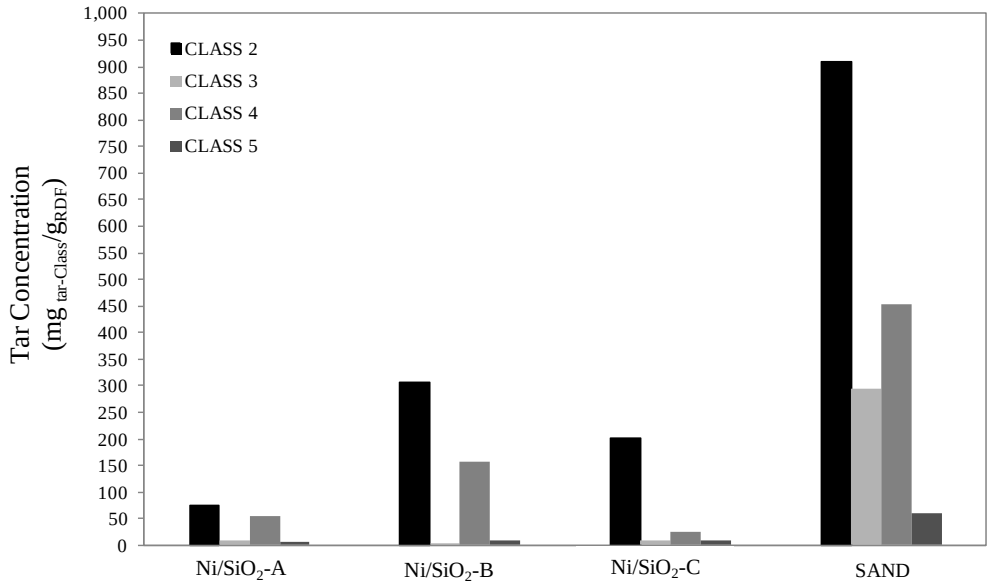

Figure 4. (a) Phenol pyrolysis and (b) formation of naphthalene and (methyl)indenes [44]

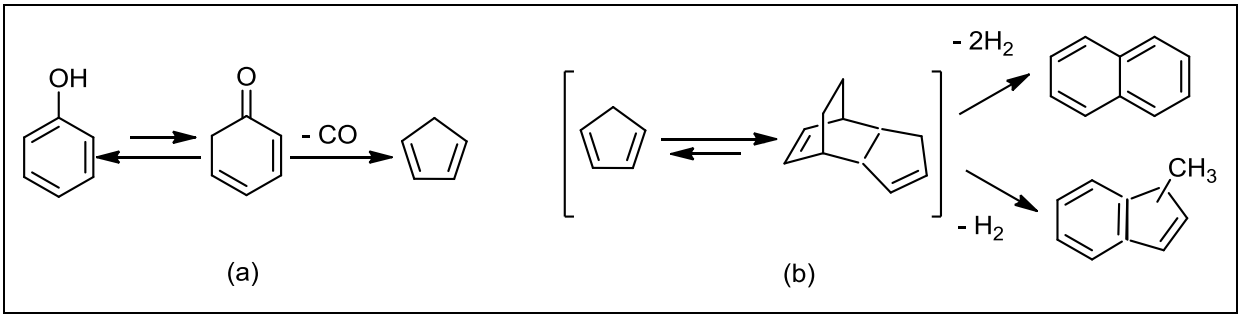

Figure 5. DTG-TPO and TGA-TPO of reacted Ni/SiO_2 catalysts

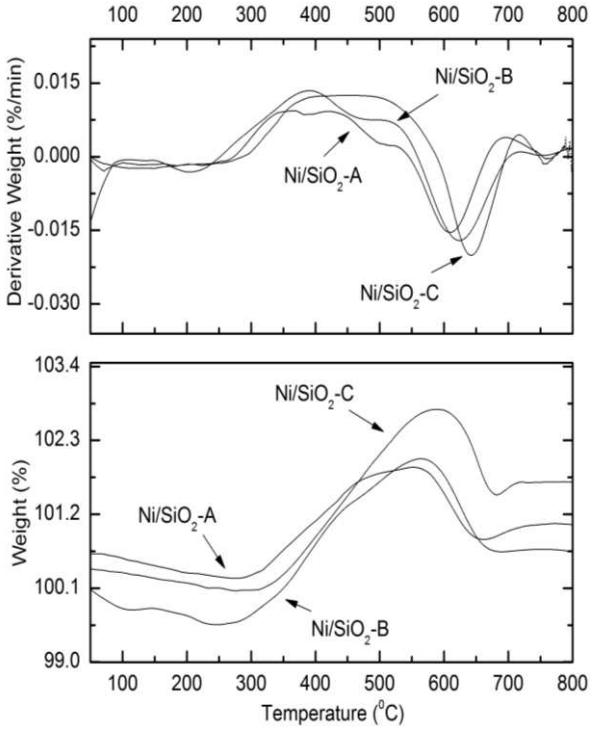

Figure 6. SEM Analysis of carbon deposition over reacted Ni/SiO_2 catalysts

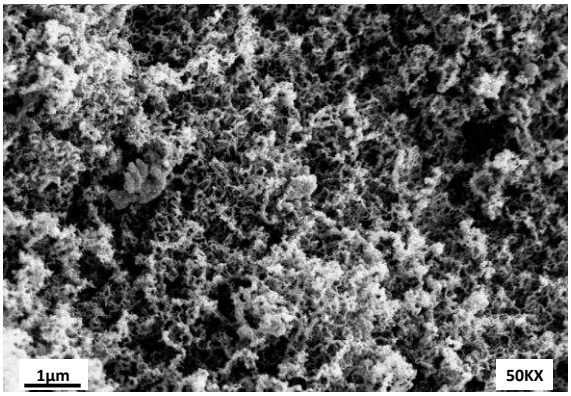

Ni/SiO_2-A (Ni:CA 1:1)

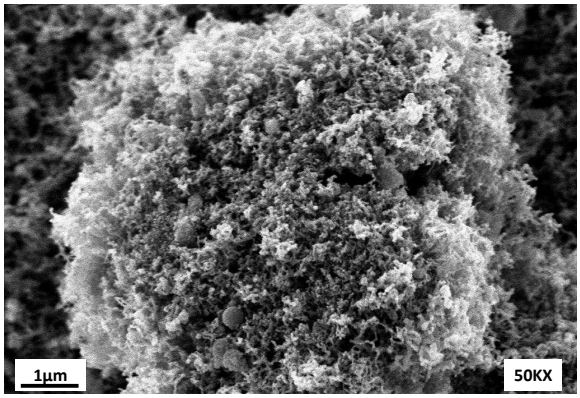

Ni/SiO_2-C (Ni:CA 1:3)